[1, *] Genghong Jiang
[2] Chao Wang
[1] Zhonghua Yao
[1] Haixuan Qiu

Research on engine multiple fault diagnosis method based on cascade model

Journal of Electrical Systems

Abstract: - The engine is the core component of the power system, and the health status of the components of the engine is very important for the normal operation of the power system. Most of the exist-ing fault diagnosis methods diagnose the engine fault type without further analysis of the sever-ity of the fault. Different fault severity requires different maintenance measures. Therefore, this paper proposes a cascading fault diagnosis model based on Gated Recurrent Unit (GRU) to di-agnose the fault type and the severity of the corresponding fault type.Firstly, the effective fea-tures are extracted from the vibration signals, and then the features are input into the GRU for fault type diagnosis to obtain the sub-fault diagnosis model. After training, one fault type diag-nosis model and four fault severity diagnosis models are obtained. Then the obtained model is cascaded to obtain the total fault diagnosis network. Fault type diagnosis is located at the first level, and four fault severity diagnosis is located at the second level. The effectiveness of the proposed method is verified by experimental data.

Keywords: Engine; Gated Recurrent Unit; Fault diagnosis.

I. INTRODUCTION

Engine is an important core component of power equipment such as internal combustion engine and compressor. Timely detection of failure types and corresponding fault severity and processing are of great significance to the normal operation of equipment, increase life safety and reduce property losses.

With the development of science and technology in recent years, artificial intelligence has made great progress. Since artificial intelligence methods do not require much professional knowledge and can achieve good diagnostic accuracy through training models, Artificial intelligence methods such as Support Vector Machine (SVM), Convolutional Neural Network (CNN), LSTM, Long short-term Memory (DAE), Denoising autoencoder (DAE) and Deep Belief Network (DBN) are widely used in fault diagnosis.

Shang[1] used signal processing methods empirical Mode decomposition (EMD) and Singular Value decomposition (SVD) for feature selection. Then the selected features were sent to SVM for classification and the classification accuracy reached 93.0%. Because the features of SVM need to be designed and extracted manually, the difficulty of fault diagnosis is increased and the features to be extracted are not flexible enough. CNN has attracted more attention from researchers due to its powerful feature extraction ability. Hu[2] proposed to input the original signals directly into CNN for feature extraction, and then input the extracted features directly into SVM for fault diagnosis. Ali Dibaj[3] uses fine-tuning Variational Mode Decomposition (VMD) and Hilbert Huang Transform (HHT) to extract time-frequency features and send them into CNN as input for fault detection. By using this method, complex fault detection of different faults with different severity is obtained. He[4] completed the fault diagnosis of bearings by using CORAL alignment and 1D-CNN for transfer learning. Qin[5] uses manual time domain features, original vibration signals and time-frequency domain features to input 1D-CNN for fault diagnosis, which is resistant to strong environmental noise and changes in operating conditions and improves diagnostic stability. DBN as a hotspot network of deep learning is also applied to fault diagnosis. Feng[6] made use of the combined complexity entropy of single signal entropy and DBN for fault diagnosis and achieved good results.However, most of the above methods only consider the spatial relationship of data but ignore the temporal relationship. The temporal relationship of mechanical equipment signal data is quite important for fault diagnosis. Therefore, it has a Recurrent Neural Network (RNN) that can reflect the temporal relationship, which plays a very important role in improving the accuracy of fault diagnosis. Li[7] diagnosed arc faults by using RNN, rapid continuous detection and probability-based classification results and achieved good diagnosis results. However, due to the RNN length dependence problems disappear and gradient, LSTM and GRU helped have been proposed to alleviate these problems. Zhao[8] used LSTM to complete the fault diagnosis of additive manufacturing equipment. Han[9] combined VAE and LSTM to form the deformation variational

[1] Zhejiang Institute of Communications, Hangzhou 311112, China
[2] Hangzhou Dianzi University, Hangzhou 310018, China
*Corresponding author: Genghong Jiang

autoencoder and conducted fault diagnosis by reconstruction error. Hao[10] used CNN and LSTM successively to extract spatial and temporal features to complete rolling bearing fault diagnosis. Qiao[11] extracted time-domain and time-frequency domain features from the original data set as inputs and sent them to CNN and LSTM to extract spatial and temporal features respectively for fault diagnosis and achieved good results. Musab ElDali[12] derived corresponding measurements using GNN (Growing Recurrent Neural Networks) and VarLSTM (Variable Sequence Long and short-term memory Neural network). The failure probability is obtained by comparing the derived and actual measured values. Compared with LSTM, GRU can alleviate the problems of gradient vanishing and length dependence of RNN and has higher computational efficiency, so it is widely used in fault diagnosis. Wang[13] used BI-GRU (bi-GRU) to complete the fault diagnosis of high voltage DIRECT current (MMC-HVDC) system of modular multilevel converter. Liu[14] first processed the original signal with short-time Fourier transform to obtain the time-frequency features, and then sent the time-frequency features into one-dimensional convolutional network and GRU successively for bearing fault diagnosis. Zhang[15] used CNN and GRU to extract time and space features respectively for fault diagnosis. Yang[16]first extracted time-frequency domain features of signals using wavelet transform, and then sent them as input to CNN and GRU for turnout fault diagnosis.

Most of the above methods are fault diagnosis methods without further classification of fault severity. These classification methods are not conducive to taking reasonable maintenance measures. Some scholars also adopted some methods to analyze the severity of faults. Xiao[17] used wavelet transform and curve fitting to obtain the warning value and alarm value, and judged the fault degree based on the fault indication value obtained by fitting. This method is highly dependent on the selection of wavelet function and requires manual determination of threshold value, and highly dependent on expert knowledge and experience. Pan[18] first carried out feature selection and dimensionality reduction, and then sent the selected features into the monotonic decision tree for fault severity diagnosis, with an accuracy of 93.58%.Jha[19]completed fault severity diagnosis of rolling bearings in two stages by using multi-classification support vector machine. Machine learning methods such as SVM can only extract shallow features and cannot well mine data information, and the generalization ability of the model is poor in the face of a large amount of data. Almounajjed[20] completed the fault severity diagnosis of short circuit between stator locks of induction motor by using mathematical model. Hang[21] completed the detection of fault severity of synchronous motor high-resistance wiring by establishing mathematical model. Taha[22] combined dissolved gas analysis and neural pattern recognition to complete the fault severity diagnosis of power transformers and achieved a diagnosis accuracy of 92.8%.Model-based fault severity diagnosis methods are difficult to implement in many cases because of the need for professional knowledge and rich experience in modeling, and the generalization ability of model-based methods is generally weak. Yang[23] used integrated learning to complete fault severity diagnosis of rolling bearings, with training accuracy of 98.57%, verification accuracy of 100%, and test accuracy of 96.51%. Gai[24] used DBN to complete the fault severity diagnosis of rolling bearings, with an average detection accuracy of 96%. The fault severity analysis of the above methods has a small number of fault severity types and is not good at solving complex problems. Sun[25] completed the diagnosis of six fault types and their corresponding four fault severity levels by using multi-attentional network combined with deep learning. However, the proposed method has high requirements on input as well as environmental variables and control variables, and these data requirements cannot be realized in many practical situations. Ali Dibaj[3] used VMD and CNN to complete the fault severity diagnosis of bearings and gears, but this method requires setting VMD parameters and selecting thresholds. Whether these parameters are reasonable or not has a great influence on the fault diagnosis results, which can only be obtained by further analysis of the results obtained from the network. Many machine learning methods (such as SVM, etc.) can only mine shallow features and their generalization ability decreases when the amount of data increases. In this paper, the RNN series network with strong capability for processing temporal data is used. Since GRU and LSTM can alleviate the gradient vanishing and length-dependent problems of RNN and have good mining capability for temporal data. Moreover, GRU has fewer network parameters than LSTM, which can greatly increase the computing efficiency. Therefore, GRU is selected as the network. Many fault severity diagnoses require that the input data content is not easy to get and the diagnosis results need to set the threshold value manually. In this paper, an intelligent diagnosis model which only needs a single vibration signal cascade network is proposed to analyze the engine faults and their severity. A two-level network is set up. The first-level network is used to diagnose the fault type, and the second-level different network model is used to diagnose the fault severity of the corresponding fault type. In this paper, the original data were firstly obtained through setting experiment and data

collection, and then the features were selected by using the double Pearson coefficient[26] and sent to the cascade network for fault type and fault severity diagnosis.

The structure of this paper is as follows. The second chapter introduces the principle, the third chapter describes the data set and fault methods, the fourth chapter describes the experimental results, and the fifth chapter summarizes.

II. MATERIALS AND METHODS

The signal type used in the experiment in this paper is time domain signal, and the temporal sequence relationship between signal points plays an extremely important role in fault diagnosis. Therefore, this paper chooses the recurrent neural network with strong processing capability of temporal sequence data as the selected network for fault diagnosis. The recurrent neural network is divided into RNN, LSTM and GRU. RNN has the simplest structure but has the problem of gradient vanishing, while LSTM and GRU are its variants, alleviating the problem of gradient vanishing to varying degrees. Compared with GRU, LSTM has more parameters and lower computational efficiency. In this paper, GRU is selected as the network to almost achieve the same accuracy as LSTM, with fewer parameters and higher computational efficiency.

A. Gated Recurrent Unit (GRU)

RNN is a neural network used to process sequential data, however, it has limitations in that there is gradient vanishing during back propagation and the traditional RNN has only short term memory but not for problems with long term memory. Therefore, a variant of it, GRU, is chosen to be used in the paper, as shown in Figure 1 where GRU is proposed to add gates to the network to overcome the limitations in RNN.

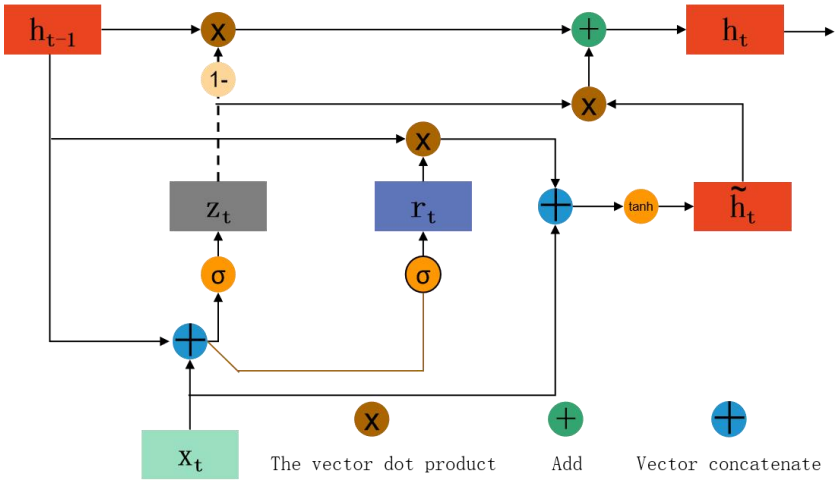

Figure 1. The GRU structure

Figure 1 shows the internal expansion structure of GRU. ht-1 represents the hidden state of the previous moment, which is historical information, h̃trepresents the candidate hidden state at the current moment, ht represents the hidden state at the current moment, xt represents the input at the current moment, rt represents the reset gate, and zt represents the update gate. The value range of rt and zt are both [0, 1]. The value of rt represents the degree to which historical information is introduced into the candidate hidden state h̃t in the calculation process of the current moment. If the value of rt is close to 0, it means that historical information is completely ignored. A larger value of zt indicates that the information at the current moment uses more historical information. The specific calculation formula is shown in (1) :

$$r_t = \sigma\left(W_r\left[x_t, h_{t-1}\right] + b_r\right), \tag{1}$$

Where xt is the input at time t, Wr is the weight of rt, br is the bias of the reset gate rt, [xt, ht-1] is the concatenate of two vectors, and σ is sigmoid function. The update gate zt is used to control the proportion of historical information used during calculations. Similar to reset gate rt, the greater the value of the update gate, the greater the historical information of the loop block used. The calculation formula is shown in Equation (2) :

$$z_t = \sigma\left(W_z\left[x_t, h_{t-1}\right] + b_z\right), \tag{2}$$

Where Wz is the weight of zt, and bz is the bias of the update gate zt.

The calculation formula of hidden candidate state h̃t is shown in Equation (3) :

$$\tilde{h}_t = \tanh\left(W_{\tilde{h}}\left[x_t, \left(r_t \cdot h_{t-1}\right)\right] + b_{\tilde{h}}\right), \tag{3}$$

Where $W_{\tilde{h}}$ is the weight of $\tilde{h}t$ and $b_{\tilde{h}}$ is the offset of hidden candidate state $\tilde{h}t$.• is for the vector dot product. The calculation formula of the hidden state ht at the current moment is shown in Equation (4) :

$$h_t = \left(1 - z_t\right) \cdot h_{t-1} + z_t \cdot \tilde{h}_t, \tag{4}$$

B. Pearson correlation coefficient

Pearson correlation coefficient is widely used to measure the degree of correlation between two variables. The greater the absolute value of the correlation coefficient, the stronger the correlation: the closer the correlation coefficient is to 1 or -1, the stronger the correlation; the closer the correlation coefficient is to 0, the weaker the correlation. In this paper, Pearson correlation coefficient is used to select features for fault diagnosis. Assuming that the data of two time series data segments A and B are A=(a1, a2, a3……an), B=(b1, b2, b3……bn), and n represent the length of data segments, Pearson correlation coefficient ρA, B between the two sets of data can be calculated as formula (5) :

$$\rho_{A,B} = \frac{\operatorname{cov}\left(A, B\right)}{\sigma_A \sigma_B} = \frac{E\left[\left(A - \mu_A\right)\left(B - \mu_B\right)\right]}{\sigma_A \sigma_B}, \tag{5}$$

σA, σB, μA and μB are the mean and variance of A and B, respectively.

C. Feature extraction and data enhancement

The variation coefficient of cylinder head vibration signal was selected as the selected feature by using the double Pearson coefficient. Then, in order to prevent over-fitting due to the small amount of data, the variation coefficient was enhanced by using the sliding window method. The sliding window step was selected as 4, and the window length was selected as 128.

D. The diagnosis process

GRU is used as the network of choice because it not only mines the temporal features in the data, but also alleviates the gradient vanishing and length-dependent problems of RNN, and also has fewer parameters and higher computational efficiency than LSTM. The structure of the network model used in the experiment is shown in Figure 2.

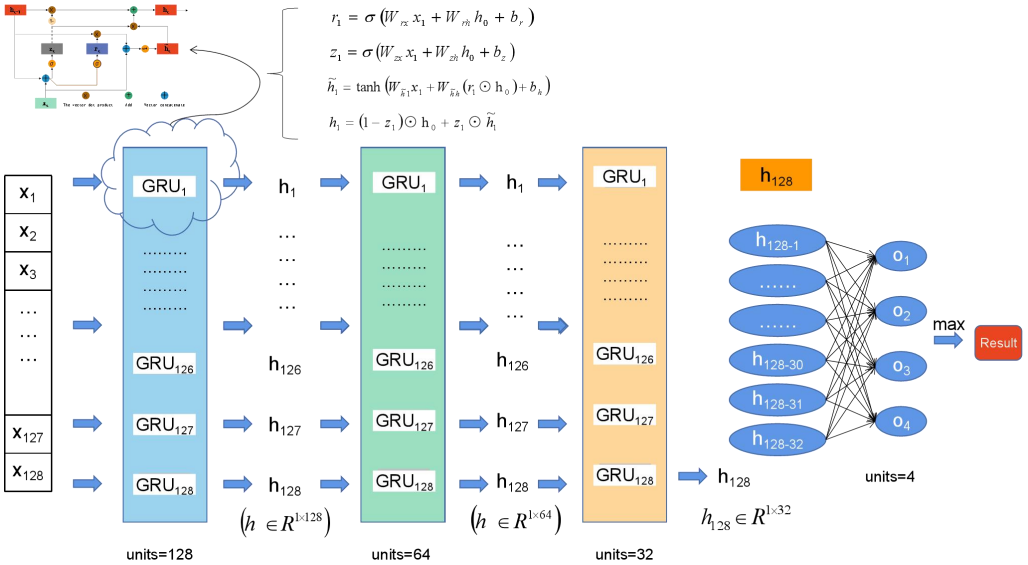

Figure 2. Network diagnosis model

The model training steps are as follows:

Step 1: The extracted features are divided into training set, validation set and test set, and then the training set and test set are fed into the network as input for model training

Step 2: Validation of the trained model using the test set

Step 3: Use the above steps to train the fault type diagnosis and fault severity diagnosis models to obtain a first-level fault type diagnosis model and four second-level fault severity diagnosis models

Step 4: Cascade the fault diagnosis model trained in the above steps. The fault type diagnostic model is at the first level, and the second level is the fault severity model

The Overall cascade model is shown in Figure 3.

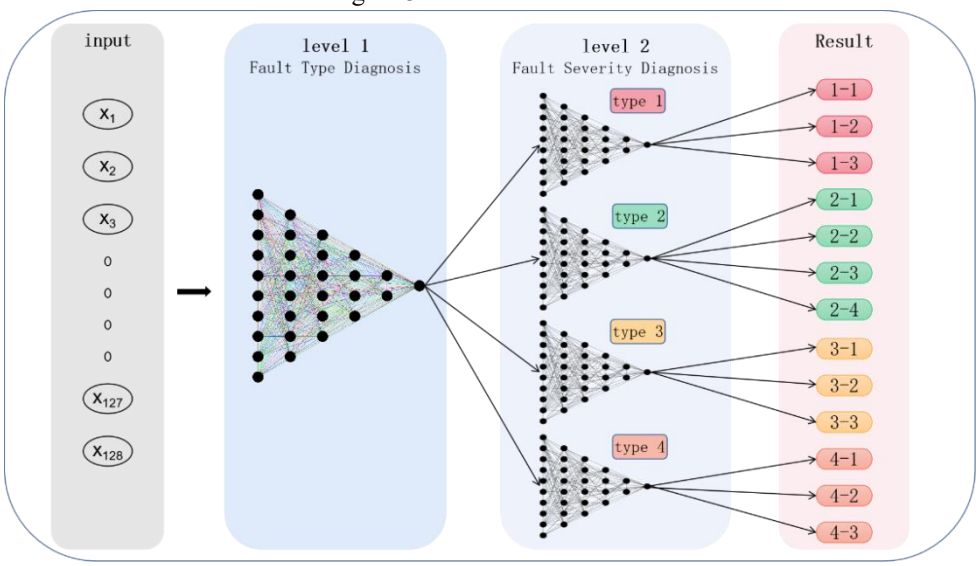

Figure 3. The Overall cascade model

III. EXPERIMENTAL VERIFICATION AND RESULT ANALYSIS

A. Experimental platform construction and data collection

In order to verify the effectiveness of the proposed method, signals collected by the fault simulation test bench are used for fault diagnosis. The fault simulation test bench for high-speed machine is composed of diesel engine, drive shaft, DC motor, console and related accessories, and its schematic diagram is shown in Figure 4.

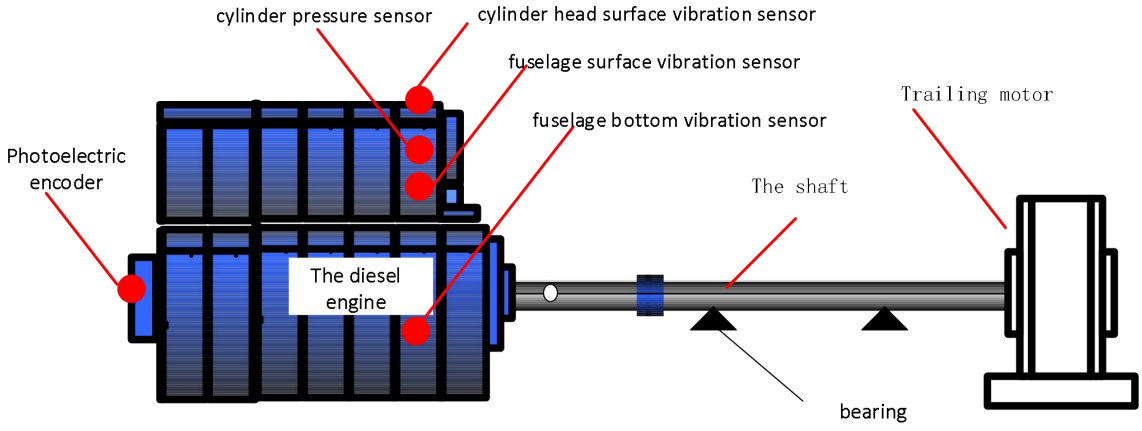

Figure 4. Schematic diagram of the failure simulation test bench

A certain type of diesel engine was selected for the test, using ECU and electronic control high pressure common rail technology, four-stroke 6-cylinder, water-cooled, in-line, dry cylinder liner type.

The signals measured in the test include cylinder head surface vibration signal, fuselage surface vibration signal, fuselage bottom vibration signal and cylinder pressure signal. Wherein, the cylinder pressure sensor is installed in the position of cylinder no. 6. In order to make the measured vibration signal as much as possible to reflect the cylinder pressure excitation, reduce the interference of other factors, the vibration acceleration sensor is installed above the cylinder head to measure the vibration signal, and the fuselage vibration signal measuring point is set in the middle of the fuselage surface.

The experimental data set is described in Table 1.

Table 1. The experimental data set

Fault Type Label	Fault Type	wear loss	Fault severity label
1	Exhaust valve wear	0mm	1-1
		0.4mm	1-2
		0.7mm	1-3
2	Cylinder wear	0.2mm	2-1
		0.4mm	2-2
		0.6mm	2-3
		0.8mm	2-4
3	Piston ring wear	1.0mm	3-1
		2.0mm	3-2
		3.0mm	3-3
4	Intake valve wear	0mm	4-1
		0.5mm	4-2
		0.8mm	4-3

B. Experiments and Results discuss

The variation coefficient of cylinder head vibration signal is selected by using Pearson correlation coefficient. After that, the sliding window method was used for data enhancement. After that, 80% of the data was selected as the training set, 20% as the verification set, and the data in the middle of the sliding step of the sliding window method was used as the test set.

The training set and verification set are sent to the neural network for training. After training, five models were obtained for fault type detection and fault severity detection of four fault types respectively. Then, the test set was used to test the trained model to verify its generalization ability. In order to prevent the interference of random factors, five different data sequence experiments were carried out for different models.

1) Parameters of cascade network model

The first-level fault type diagnosis model selects GRU as the selection network, in which three layers of GRU are used for advanced feature extraction. The number of hidden elements in the first layer is 128, and the number of hidden elements in the next two layers is 64 and 32 respectively. The output of the fully connected layer is (4,1). The dropout rate is 0.2, the Adam optimizer is used in the optimizer, and the cross entropy loss function is used in the loss function.

Adam optimization algorithm designs independent adaptive learning rates for different parameters by calculating the first and second order estimates of gradients.

First, the attenuation average of the first-order moment estimator mt and the second-order moment estimator vt are calculated by formulas (6) and (7).

$$m_t = \beta_1 \times m_{t-1} + (1-\beta_1) \times g_t , \tag{6}$$

$$\mathrm{v}_t = \beta_2 \times \mathrm{v}_{t-1} + (1-\beta_2) \times g_t^{\,2} , \tag{7}$$

β1=0.9 is the exponential decay rate of the first-order moment estimation, β2=0.999 is the exponential decay rate of the second-order moment estimation, and gt is the gradient. In the second step, the deviation is corrected. Through calculating the deviation, the first-order moment estimation and the second-order moment estimation are corrected. The correction formulas are shown in (8) and (9).

$$\hat{m}_t = \frac{m_t}{1-\beta_1^{\,t}} , \tag{8}$$

$$\hat{\mathrm{v}}_t = \frac{\mathrm{v}_t}{1-\beta_2^{\,t}} , \tag{9}$$

Parameter updates are shown in (10):

$$w_{t+1} = w_t - \frac{\alpha \times \hat{m}_t}{\sqrt{\hat{v}_t} + \varepsilon} \quad (10)$$

Wt, Wt+1 is the model parameter vector at time t and time t +1, α is the learning rate, and ε =10-8 prevents the denominator from being 0.

Cross entropy loss function:

The cross-entropy loss function can be shown in Formula (11).

$$L\left(f, \tilde{f}\right) = -\sum_x f \ln \tilde{f} \quad (11)$$

f and f̃ are the actual labels' one-hot codes and predicted probabilities, respectively.

The fault severity diagnosis model of exhaust valve, piston ring and intake valve also uses GRU as the selection network, in which three layers of GRU are used for advanced feature extraction. The number of hidden elements in the first layer is 128, and the number of hidden elements in the next two layers is 64 and 32 respectively, and the dropout rate is 0.2. The Adam optimizer is used in the optimizer. The cross entropy loss function is used in the loss function. Since the severity of these three kinds of faults can be divided into three kinds, the output shape of the full connection layer is (3,1).

According to the analysis of the experimental results, when the dropout rate is 0.5, the cylinder fault severity diagnosis model has the highest accuracy, and the dropout rate of the cylinder fault severity diagnosis model is 0.5. Meanwhile, since there are four kinds of cylinder fault severity, the output shape of the full connection layer is (4,1).

Table 2. Fault Type Diagnosis Network structure parameters

Structure	Input	Ouput	Hidden elements	The activation function
Input	(128, 1)	(128, 1)		
GRU_1	(128, 1)	(128, 128)	128	Tanh
Dropout	(128, 128)	(128, 128)		
GRU_2	(128, 128)	(128, 64)	64	Tanh
Dropout	(128, 64)	(128, 64)		
GRU_3	(128, 64)	(128, 32)	32	Tanh
Dense	(16, 1)	(4, 1)		Softmax

Then, the weight and bias parameters of each model are obtained through corresponding data training. Fault Type Diagnosis Network structure parameters are shown in Table 2.

The cascade model is used to simplify the problems. The fault type diagnosis model is used to diagnose the four fault types. After the fault type diagnosis is completed, the fault severity diagnosis model is selected to diagnose the corresponding fault severity. There are four fault severity diagnosis models, which are used to diagnose different wear degrees of piston ring, intake valve, exhaust valve and cylinder respectively.

2) Fault type diagnosis

The TSNE dimension reduction representation of the test set confusion matrix and network extracted features of a random experiment for fault type diagnosis is shown in Figure 5. It can be seen from the figure that the diagnosis results of the model for the test set data that did not participate in the training model are all correct, which shows that the model has good generalization ability. The training accuracy of the five random experiments reached 100%, and there were two misdiagnosis cases in each experiment, with an average test accuracy of 99.99%. The figure shows the T-SNE dimensional-reduction representation of the 32-dimensional features of the first full-connection layer of the fault type diagnosis model of the cascading model. Since fault diagnosis is a data set containing 13 kinds of fault severity data, it is difficult to classify the data. It can be seen from the figure that although there is a class of fault features that are not well aggregated, However, there is no intersection between the features of different fault types, and better classification results can still be achieved.

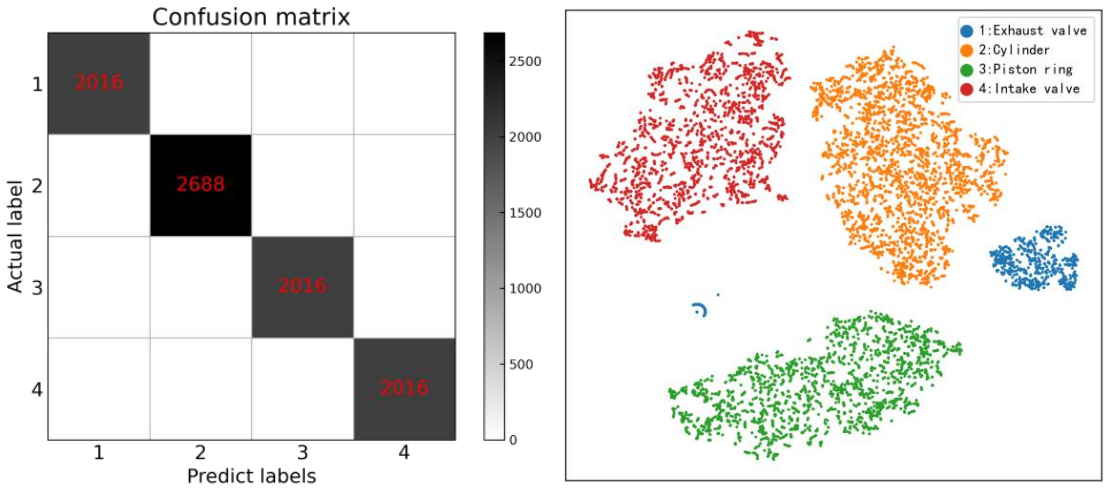

(a) (b)

Figure 5. The fault type diagnostic test set (a) confusion matrix and (b) T-SNE features

3) Fault severity diagnosis of exhaust valve, piston ring and intake valve

The exhaust valve, piston ring and intake valve all have three fault severity degrees. The corresponding fault severity diagnosis test set confusion matrix and TSNE dimensionality reduction of network extraction features are shown in Figure 6, Figure 7, Figure 8. It can be seen from the confusion matrix of the three models that the test accuracy of the model graph has reached 100%, and the generalization ability of the model has been verified. The figure shows the T-SNE dimensionality reduction of the 32-dimensional feature of the first full-connection layer of the cascading model's fault severity diagnosis model for piston rings, intake valves and exhaust valves. The fault types of these three faults are all three, indicating that the data features of different fault severity are obviously distinguished. In the five random experiments of the fault severity of the three fault types, only the exhaust valve had one misdiagnosis in the test set diagnosis, and the accuracy of the test set diagnosis in the five random experiments of the other two fault types was 100%.

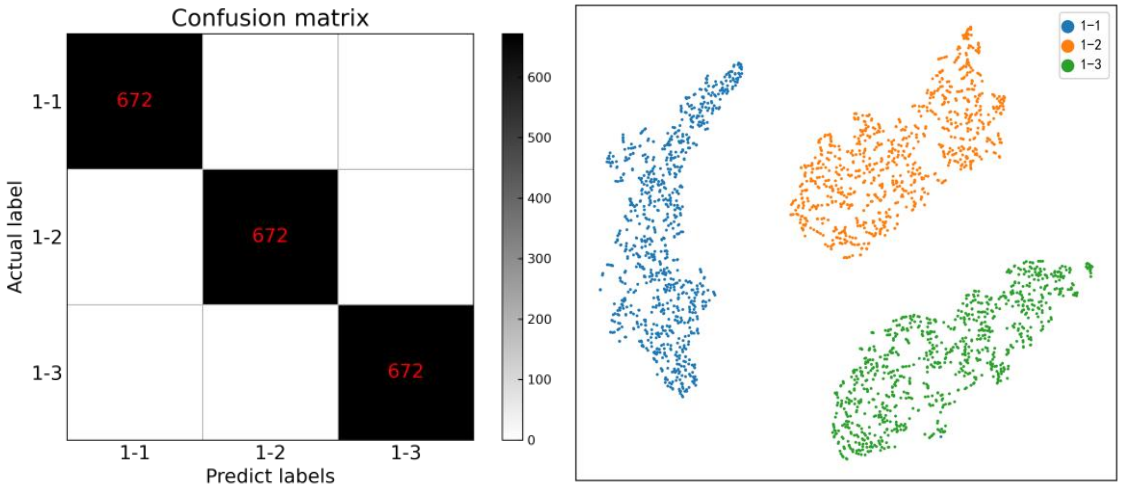

(a) (b)

Figure 6. The exhaust valve fault severity test set (a) confusion matrix and (b) T-SNE features

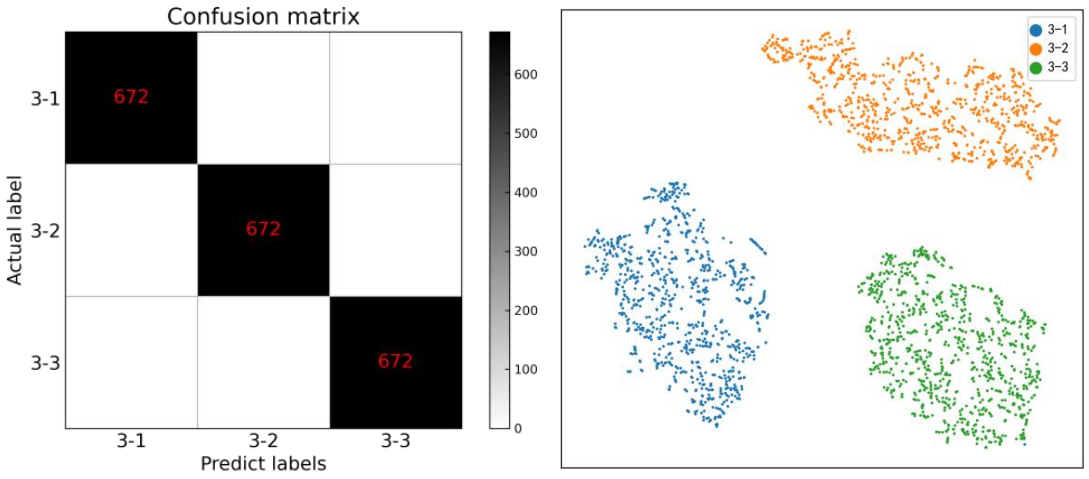

(a) (b)

Figure 7. The piston ring fault severity test set (a) confusion matrix and (b) T-SNE features

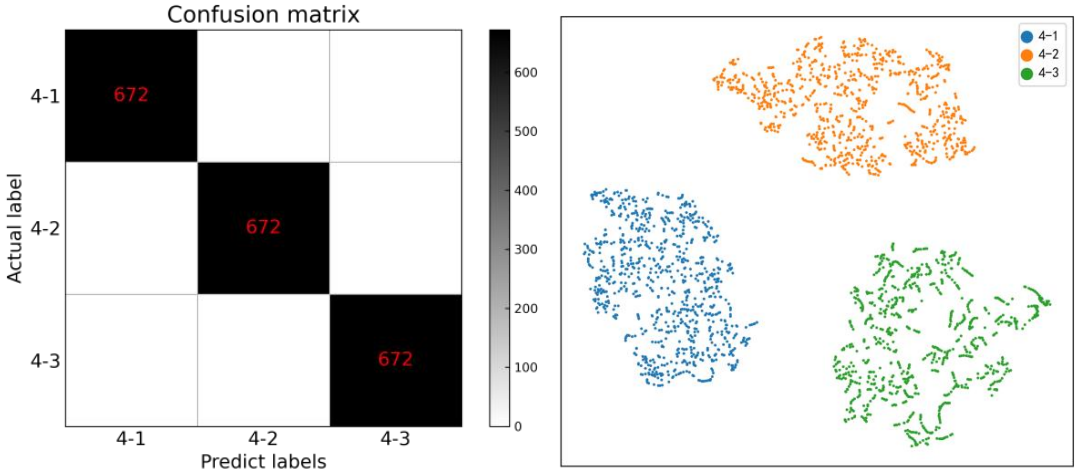

(a) (b)

Figure 8. The intake valve fault severity test set (a)confusion matrix and (b)T-SNE features

4) Fault severity diagnosis of cylinder

There are four kinds of cylinder fault severity, which is more difficult to diagnose than the other three types of fault. Cylinder fault severity diagnosis test set confusion matrix and features extracted from the network are represented by TSNE dimensionality reduction as shown in Figure 9. The t-SNE dimensionality reduction representation of 32-dimensional features of the first full-connection layer of the cylinder fault severity diagnosis model for the cascade model is shown below. There are four fault states for cylinder fault diagnosis. Compared with the other three fault severity diagnosis models, the diagnosis is more difficult. However, it can be seen from the figure that the classification features of different types of faults are clearly distinguished, which can achieve the purpose of classification. In the process of testing the generalization ability of test set for fault severity diagnosis of cylinder, only one instance of random experiment was misdiagnosed, and the remaining instances were correct, and the average test accuracy reached 99.99%.

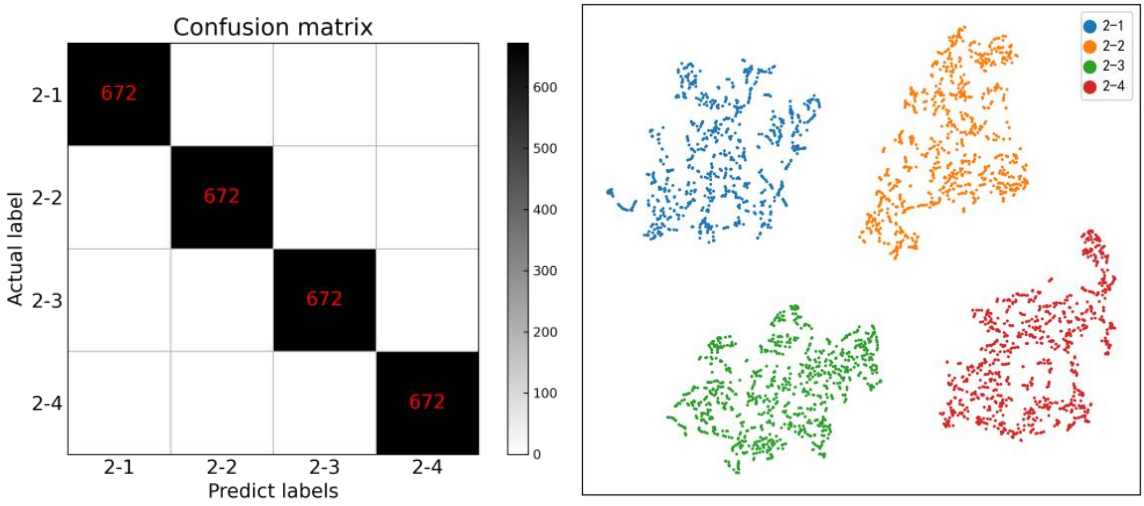

(a) (b)

Figure 9. The cylinder fault severity test set (a) confusion matrix and (b) T-SNE features

5) Diagnosis accuracy analysis of cascaded network model

The test accuracy of fault type diagnosis model is up to 99.99%. In the fault severity diagnosis model, the test accuracy of piston ring fault severity diagnosis is 100%, the test accuracy of intake valve fault severity diagnosis is 100%, the test accuracy of exhaust valve fault severity diagnosis is 99.99%, the test accuracy of cylinder fault severity diagnosis is 99.99%. The engine fault type and severity can be diagnosed by the cascade of fault severity diagnosis and fault diagnosis model. The accuracy of the cascaded network fault diagnosis model is 99.99%. Compared with Pan [18], which used monochromatic decision tree to diagnose fault severity and achieved 93.58% accuracy, and Taha [22], which combined dissolved gas analysis and neural pattern recognition to complete fault severity diagnosis of power transformer and achieved 92.8% diagnosis accuracy, achieved higher accuracy.

6) Analysis of the impact of dropout rates on the accuracy of network model

If dropout rate is too large, the model will be Underfitting and the accuracy will be reduced, while if the loss rate is too small, the model will be overfitting and the model generalization ability will be weak. In order to select a reasonable loss rate, By adopting four dropout rates of 0.2, 0.3, 0.4 and 0.5 for fault type diagnosis model and fault severity diagnosis model, reasonable model parameters can be obtained.

Table 3 shows the accuracy of the fault type diagnosis model with different dropout rates. It can be seen that when the dropout rate of the model is 0.2, the average training accuracy and average verification accuracy of the model's five random tests are 100%, and the average test accuracy is 99.99%, which is higher than the other three dropout rates. Moreover, it can be seen that the accuracy decreases with the increase of the loss rate, indicating that the model has better performance when the loss rate is 0.2, and the increase will lead to the underfitting of the model.

Table 3. The accuracy of the fault type diagnosis model with different dropout rates

Dropout rate	Average training accuracy	Average verification accuracy	Average test accuracy
0.2	100.00%	100.00%	99.99%
0.3	100.00%	100.00%	99.98%
0.4	99.96%	100.00%	99.64%
0.5	99.97%	99.63%	99.87%

Table 4. The diagnostic model accuracy of exhaust valve fault severity with different dropout rates

Dropout rate	Average training accuracy	Average verification accuracy	Average test accuracy
0.2	100.00%	100.00%	99.99%
0.3	100.00%	100.00%	99.98%
0.4	100.00%	100.00%	99.87%
0.5	100.00%	100.00%	99.95%

Table 5. The diagnostic model accuracy of cylinder fault severity with different dropout rates

Dropout rate	Average training accuracy	Average verification accuracy	Average test accuracy
0.2	100.00%	99.84%	99.89%
0.3	100.00%	99.99%	100.00%
0.4	100.00%	99.94%	100.00%
0.5	100.00%	99.99%	100.00%

Table 6. The diagnosis model accuracy of piston ring fault severity with different dropout rates

Dropout rate	Average training accuracy	Average verification accuracy	Average test accuracy
0.2	100.00%	100.00%	100.00%
0.3	100.00%	100.00%	99.99%
0.4	100.00%	100.00%	99.84%
0.5	100.00%	99.85%	99.89%

Table 7. The diagnostic model accuracy of intake valve failure severity with different dropout rates

Dropout rate	Average training accuracy	Average verification accuracy	Average test accuracy
0.2	100.00%	100.00%	100.00%
0.3	99.70%	99.96%	99.82%
0.4	99.78%	100.00%	99.85%
0.5	99.81%	99.85%	99.80%

Table 4 shows the diagnostic model accuracy of exhaust valve fault severity with different dropout rates. It can be seen that when the dropout rate of the model is 0.2, the average test accuracy of the five random tests of the model is 99.99%, which is higher than the other three loss rates and has the strongest generalization ability, indicating that the model has better performance when the dropout rate is 0.2. The selected parameters are reasonable.

Table **5** shows the diagnostic model accuracy of cylinder fault severity with different dropout rates. It can be seen that when the dropout rate of the model is 0.3 and 0.5, the average test accuracy of the model's five random tests is 100%, and the average verification accuracy is 99.99%, which is higher than the accuracy of other loss rates. It shows that the loss rate of model selection is reasonable.

Table 6 shows the diagnosis model accuracy of piston ring fault severity with different dropout rates. It can be seen that when the dropout rate of the model is 0.2, the average test accuracy, average verification accuracy and average training accuracy of the five random tests of the model are 100%, which is higher than the accuracy of other loss rates. Moreover, the overall accuracy of the model decreases with the increase of the dropout rate, indicating that the optimal performance is achieved when the dropout rate is set to 0.2, and the increase of dropout rate leads to under-fitting.

Table 7 shows the diagnostic model accuracy of intake valve failure severity with different dropout rates. It can be seen that when the dropout rate of the model is 0.2, the average test accuracy, average verification accuracy and average training accuracy of the five random tests of the model are 100%, which is higher than other dropout rates. The dropout rate of the model is reasonable.

IV. CONCLUSION

The detection of equipment fault types and corresponding fault severity plays an extremely important role in timely taking reasonable maintenance measures to protect life and reduce production costs. Most of the existing methods are fault diagnosis. However, some fault severity diagnosis methods have some problems, such as less fault types and corresponding degrees, simpler problems, higher input requirements, and multiple parameters need to be determined according to experience.

In this paper, the fault type and severity of engine are diagnosed by using cascade network combined with GRU. In this paper, the fault type is firstly diagnosed by using the first-level network, and then the fault severity diagnosis model is used to diagnose the fault severity according to the corresponding fault type. Experimental results show that the proposed method achieves good accuracy, and the effectiveness of the proposed method is verified.

In the following research, we will focus on the transfer learning of this method and the maximum number of faults that can be diagnosed so that this method can be applied in other fields and create greater economic benefits.

FUNDING:

This work is supported by the "Pioneer" and "Leading Goose" R&D Program of Zhejiang (Grant no. 2023C03154).

DATA AVAILABILITY STATEMENT:

Not applicable.

ACKNOWLEDGMENTS:

The authors acknowledge funding from the National Natural Science Foundation of China.

CONFLICTS OF INTEREST:

The authors declare no conflict of interest.

REFERENCES

[1] Xueyi S.; Xibing L.; Kang P.; Longjun D.; Zewei W., Feature extraction and classification of mine microseism and blast based on EMD-SVD. Chinese Journal of Geotechnical Engineering 2016, 38, (10), 1849-1858.

[2] Xiaoyi H.; Yunjian J.; Zhikun S.; Yinqing H., Bearing fault identification by using deep convolution neural networks based on CNN-SVM. Journal of Vibration and Shock 2019, 38, (18), 173-178.

[3] Dibaj, A.; Ettefagh, M. M.; Hassannejad, R.; Ehghaghi, M. B., A hybrid fine-tuned VMD and CNN scheme for untrained compound fault diagnosis of rotating machinery with unequal-severity faults. Expert Systems with Applications 2021, 167, 114094.

[4] He, J.; Li, X.; Chen, Y.; Chen, D.; Guo, J.; Zhou, Y., Deep Transfer Learning Method Based on 1D-CNN for Bearing Fault Diagnosis. Shock and Vibration 2021, 2021, 1-16.

[5] Qin, C.; Jin, Y.; Tao, J.; Xiao, D.; Yu, H.; Liu, C.; Shi, G.; Lei, J.; Liu, C., DTCNNMI: A deep twin convolutional neural networks with multi-domain inputs for strongly noisy diesel engine misfire detection. Measurement 2021, 180, 109548.

[6] Feng, D.; Xiao, M.; Liu, Y.; Song, H.; Yang, Z.; Hu, Z., Finite-sensor fault-diagnosis simulation study of gas turbine engine using information entropy and deep belief networks. Frontiers of Information Technology & Electronic Engineering 2016, 17, (12), 1287-1304.

[7] Li, W.; Liu, Y.; Li, Y.; Guo, F., Series Arc Fault Diagnosis and Line Selection Method Based on Recurrent Neural Network. IEEE Access 2020, 8, 177815-177822.

[8] Zhao, Y.; Zhang, Y.; Wang, W. In Research on condition monitoring of FDM equipment based on LSTM, 2021, 2021; IEEE: 2021; pp 612-615.

[9] Han, P.; Ellefsen, A. L.; Li, G.; Holmeset, F. T.; Zhang, H., Fault Detection With LSTM-Based Variational Autoencoder for Maritime Components. IEEE Sensors Journal 2021, 21, (19), 21903-21912.

[10] Hao, S.; Ge, F.; Li, Y.; Jiang, J., Multisensor bearing fault diagnosis based on one-dimensional convolutional long short-term memory networks. Measurement 2020, 159, 107802.

[11] Qiao, M.; Yan, S.; Tang, X.; Xu, C., Deep Convolutional and LSTM Recurrent Neural Networks for Rolling Bearing Fault Diagnosis Under Strong Noises and Variable Loads. IEEE Access 2020, 8, 66257-66269.

[12] ElDali, M.; Kumar, K. D. In Fault Diagnosis and Prognosis of Aerospace Systems Using Growing Recurrent Neural Networks and LSTM, 2021, 2021; IEEE: 2021; pp 1-20.

[13] Wang, Y.; Zheng, D.; Jia, R., Fault Diagnosis Method for MMC-HVDC Based on Bi-GRU Neural Network. Energies 2022, 15, (3), 994.

[14] Liu, S.; Shen, C.; Chen, Z.; Huang, W.; Zhu, Z., A sudden fault detection network based on Time-sensitive gated recurrent units for bearings. Measurement 2021, 186, 110214.

[15] Long Z.; Canzhuang Z.; Jianyu Y.; Binghuan C.; Tianpeng X.; Wenhao Y., Dual-channel feature fusion CNN-GRU gearbox fault diagnosis. Journal of Vibration and Shock 2021, 40, (19), 239-245.

[16] Juhua Y.; Yijian Y.; Guangwu C.; Yongbo S.; Dongfeng X., Research on Turnout Fault Dia g nosis Al g orithms Based on CNN-GRU Mode. Journal of the China Railway Society 2020, 42, (07), 102-109.

[17] Xiao, X.; Chai, L.; Sheng, Y. In Fault severity diagnosis of squirrel-cage induction motors in transient regime based on curve fitting, 2017, 2017; IEEE: 2017; pp 1825-1830.

[18] Pan, W.; He, H. In An Intelligent Fault Severity Diagnosis Method based on Hybrid Ordinal Classification, 2020, 2020; IEEE: 2020; pp 2414-2417.

[19] Jha, R. K.; Swami, P. D., Fault diagnosis and severity analysis of rolling bearings using vibration image texture enhancement and multiclass support vector machines. Applied Acoustics 2021, 182, 108243.

[20] Almounajjed, A.; Sahoo, A. K.; Kumar, M. K., Diagnosis of stator fault severity in induction motor based on discrete wavelet analysis. Measurement 2021, 182, 109780.
[21] Hang, J.; Li, Y.; Ding, S.; Tang, C.; Wang, Q. In High-resistance connection fault severity detection in a permanent magnet synchronous machine drive system, 2017, 2017; IEEE: 2017; pp 1-4.
[22] Taha, I. B. M.; Dessouky, S. S.; Ghoneim, S. S. M., Transformer fault types and severity class prediction based on neural pattern-recognition techniques. Electric Power Systems Research 2021, 191, 106899.
[23] Yang, H.; Li, W. D.; Hu, K. X.; Liang, Y. C.; Lv, Y. Q., Deep ensemble learning with non-equivalent costs of fault severities for rolling bearing diagnostics. Journal of Manufacturing Systems 2021, 61, 249-264.
[24] Gai, J.; Zhong, K.; Du, X.; Yan, K.; Shen, J., Detection of gear fault severity based on parameter-optimized deep belief network using sparrow search algorithm. Measurement 2021, 185, 110079.
[25] Sun, Z.; Jin, H.; Xu, Y.; Li, K.; Gu, J.; Huang, Y.; Zheng, A.; Gao, X.; Shen, X., Severity-insensitive fault diagnosis method for heat pump systems based on improved benchmark model and data scaling strategy. Energy and Buildings 2022, 256, 111733.
[26] Wang, C.; Chen, J.; Zeng, R. In An analysis and forecasts of online product sales based on BP Neural Network and Pearson Coefficient, 2020, 2020; IEEE: 2020; pp 559-564.